

Effect of pH on Structural, Electrochemical and Photoelectrocatalytic Degradation Properties of Methyl Orange

ZULKARNAIN ZAINAL*, CHONG YONG LEE, MOHD ZOBIR HUSSEIN,
ANUAR KASSIM and NOR AZAH YUSOF

*Department of Chemistry, Universiti Putra Malaysia
43400 UPM Serdang, Selangor, Malaysia*

E-mail: zulkar@fsas.upm.edu.my; Tel: (603)89466810; Fax: (603)89435380

Photoelectrocatalytic degradation of methyl orange at different pH has been studied using TiO₂ thin films. The dye structures in acidic, near neutral and basic media were analyzed using UV-Vis spectrophotometer and FTIR spectrometer. Protonation of azo group altered the dye structure from benzenoid in neutral or alkaline solution to quinoid in acidic medium. Cyclic voltammetry was employed to study the electrochemical characteristics of methyl orange at different pH. It was found that the flat-band potential shifted to more negative potential for the increase of solution pH. The photoelectrocatalytic degradation of methyl orange was found to follow the Langmuir-Hinshelwood pseudo first order kinetic model for all the pH. Solutions at pH 6 exhibited the highest degradation rate followed by pH 3, 9 and 12. The addition of supporting electrolyte increased the photodegradation rate but did not affect the trend. Supporting electrolyte was found to play an essential role in providing the conducting medium and buffering the solution.

Key Words: Photoelectrocatalytic, pH, Methyl orange, TiO₂, Supporting electrolyte.

INTRODUCTION

Azo dyes represent the largest group of dyes used in the textile industry¹; therefore the discharge of these types of effluents after the textile finishing processes are an important source of environmental contamination. Effluents containing azo dyes are found to be non-biodegradable and also resistant to destruction by physico-chemical treatment methods². In addition, they also resist aerobic degradation and under anaerobic conditions they can be reduced to potentially carcinogenic aromatic amines³. As a consequence, it is necessary to find a suitable and effective method to treat these dyes.

The emergence of heterogeneous photocatalysis process for the treatment of wastewaters provided another alternative to complement existing conventional methods. Basically, this process involves irradiation of semiconductor in aqueous solutions which induce the generation of very reactive species such as hydroxyl radicals that could quickly and non-selectively oxidize or reduce a broad range of

organic pollutants⁴⁻⁶. Among the semiconductors, TiO₂ is the most widely investigated and tremendous research works have proved its ability for complete mineralization of varieties of aqueous pollutants⁷⁻⁹.

Mainly, photocatalyst degradation using TiO₂ was investigated under suspension and immobilized systems. Nevertheless, there are many inherent problems in using the TiO₂ particle suspension. These include the difficulty of separating the photocatalyst from water, the need to replenish oxygen and the low quantum efficiency mainly resulting from inefficient separation of photogenerated charge carriers^{10, 11}. To overcome these problems, by immobilizing TiO₂ particles on to conducting substrates, photoelectrochemical techniques can be applied where the separation of photogenerated electrons and holes is accelerated and thus the recombination of photogenerated electrons and holes is suppressed.

Several studies¹²⁻¹⁵ have dealt with the investigation of various parameters on various kinds of pollutants in the electrochemical assisted photodegradation system. Acidity of the solution is generally considered to be an important parameter in determining the photodegradation efficiency. It is expected that every reactive species in different solutions has its own optimum pH range. However, it is important to understand to what extent and how this parameter affects the photodegradation process. This paper focuses on the effect of pH in photoelectrocatalytic degradation of an azo dye, methyl orange. The structural and electrochemical characteristics of this dye under different pH were investigated. Besides that, the influence of solution pH towards photoelectrocatalytic degradation in the presence and absence of supporting electrolyte was evaluated.

EXPERIMENTAL

All chemicals, tetraisopropyl orthotitanate (> 98% Ti, Merck-Schuchardt), ethanol (A.R. grade, R.G. HmbG Chemical), diethanolamine (Acros Organics), polyethylene glycol (m.w. = 2000, Fluka Chemika) and methyl orange (BDH Chemicals Ltd.) were used without further purification. All solutions in this experiment were prepared using the deionized water (Millipore Alpha-Q system, 18.2 MΩ cm).

Preparation of precursor sol: The precursor solution for TiO₂ sol was prepared using the system that contained tetraisopropyl orthotitanate, polyethylene glycol, diethanolamine, ethanol and water as reported by Kato¹⁶⁻¹⁸. Modifications were made on chemical molar ratio and adding sequences. The molarity of alkoxide in ethanol was 0.94 mol/dm³. The molar ratio of diethanolamine to the alkoxide was 1. The concentration of polyethylene glycol and water to alkoxide was 6 and 0.8 wt. %, respectively. The polyethylene glycol solution was dissolved in ethanol solution before adding other chemicals in the following sequence: diethanolamine, tetraisopropyl orthotitanate and water. The mixture was stirred in a sealed condition for several hours at room temperature. The resulting sol gel was clear and transparent.

Preparation of TiO₂ electrodes: The titanium plates (5 × 2 cm²) were used as the conducting support material for the preparation of TiO₂ electrode. The plate was polished by silicon carbide paper (bioanalytical system PK-4 polishing kit)

and later cleaned with acetone in an ultrasonic bath for 15 min. The treated Ti plate was dried in an oven at 100°C for 15 min and then dip-coated with sol-gel solution and left to dry at room temperature. The coated electrode was heated at 100°C for 5 min in oven followed by subsequent dip-coatings. An area with size $1.5 \times 2.0 \text{ cm}^2$ at the top was left uncoated to provide the area for electrical connections. This step was repeated several times until the amount of TiO_2 catalyst loaded was *ca.* 2 mg. Finally, the plate was annealed at 500°C in a Thermolyne 21100 furnace for 2 h.

FTIR characterization: The methyl orange solutions (1000 ppm) were prepared at pH 3, 6, 9 and 12 by adding sodium hydroxide or hydrochloric acid. The dried methyl orange powders were obtained by drying the prepared methyl orange solution at 100°C in an oven for 12 h. The powders were analyzed using FTIR spectrometer model 1725X. The dried methyl orange was ground into fine powder together with potassium bromide. The ground powder was compressed into a pellet using a pellet compressor. A non-transparent pellet suitable for the analysis was obtained.

Voltammetrics and photoelectrocatalytic degradation studies: A potentiostat EG&G Princeton Applied Research VersaStat driven by model 270 Electrochemical Analysis System software with PC control was used for linear sweep voltammetry and cyclic voltammetry (CV) measurements. Meanwhile, the photoelectrocatalytic degradation experiments were carried out in the two-compartment cell equipped with a quartz plane window. The anode and cathode electrodes were separated by polytetrafluoroethylene 0.45 μm membrane. The working electrode was a TiO_2/Ti plate and the counter electrode was a platinum plate (1 cm^2). All the potentials were specified to the Ag/AgCl reference electrode which was connected to the assembly *via* a salt bridge. The electrode potentials and photocurrents were recorded using AMEL general-purpose potentiostat-galvanostat model 2049. All the potentials were fixed at 1.0 V during the photoelectrochemical degradation process. The temperature of the reactor solutions was maintained at 313 K throughout the experiment by using a water jacket circulation system around the cell. Tungsten halogen projector lamp (Osram, 300 W and 120 V) was used as a light source. The light source was placed 8 cm away from the sample. For photoelectrocatalytic degradation, a series of methyl orange solutions (10 ppm) at pH 3, 6, 9 and 12 were prepared with and without adding 0.1 M NaCl. Photoreactor cell was filled by an amount of 120 mL methyl orange. The samples were withdrawn every 30 min thereafter for period of 120 min. The concentration of methyl orange in the solution was determined by measuring the absorbance values using UV/Vis Perkin-Elmer Lambda 20 spectrophotometer.

RESULTS AND DISCUSSION

The chemical formula of methyl orange is $\text{NaO}_3\text{SC}_6\text{H}_4\text{N}=\text{NC}_6\text{H}_4(\text{CH}_3)_2$. It is one of the simplest azo dyes with one nitrogen double bond, one sulphonate group, one dimethylamine group and two aromatic rings.

Fig. 1 depicts the UV-Vis spectra of the dye in water at different pH: 3, 6, 9 and 12. The spectra are almost similar for three pH 6, 9 and 12 values. The

maximum adsorbance (λ_{max}) at wavelength 464.5 nm is due to the violet colour of the solutions which is attributed to the $n \rightarrow \pi^*$ transition of non-bonding nitrogen electrons to the antibonding π^* group orbital of the double bond system¹⁹. Besides that, the second group of bands, with an increasing absorbance with pH in the UV region of the spectrum is characteristic for aromatic rings²⁰.

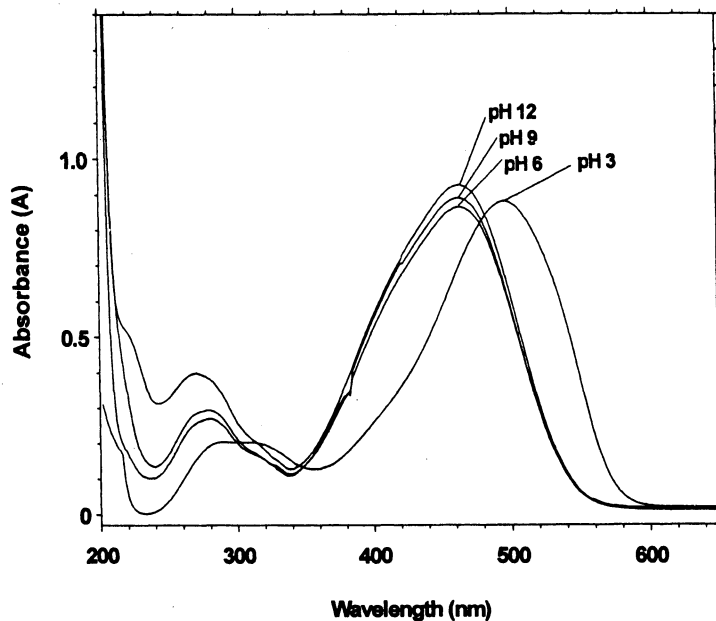


Fig. 1. UV-absorption spectra of methyl orange at pH 3, 6, 9 and 12

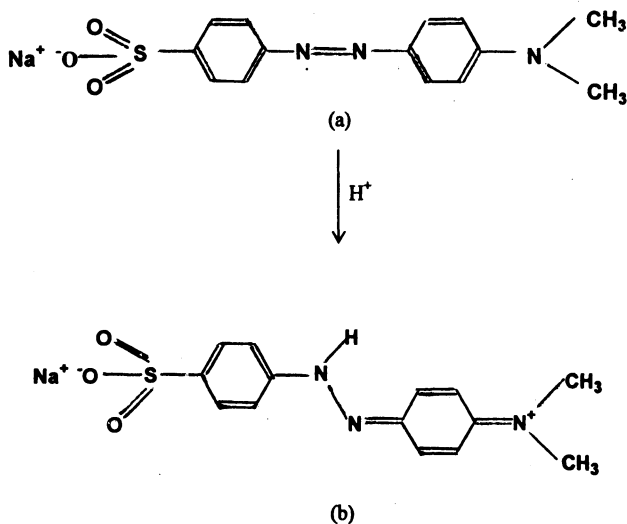


Fig. 2. Structures of methyl orange at (a) alkaline and (b) acidic pH

At acidic condition (pH 3), the spectrum exhibits a red shift where the λ_{\max} increase to 502 nm which is attributed to a change of the dye structure due to protonation. The change of the solution's colour from yellow to red by increasing acidity is another evidence for protonation²¹. Methyl orange exhibits different conjugated double bonds due to the rearrangement of these bonds in one of the benzene rings. The alkaline and acidic structures appear as shown in Fig. 2. The structures of methyl orange in alkaline and acidic conditions are referred to as benzenoid and quinoid, respectively.

Fig. 3 shows the FTIR spectrum for methyl orange solution at different pH. The characteristic vibration for unsymmetrical azo compounds which represent N=N stretching frequency occurring at 1418 cm^{-1} was found in the spectra²² for pH 6, 9 and 12. This band was non-existent on the spectrum for acid precipitate

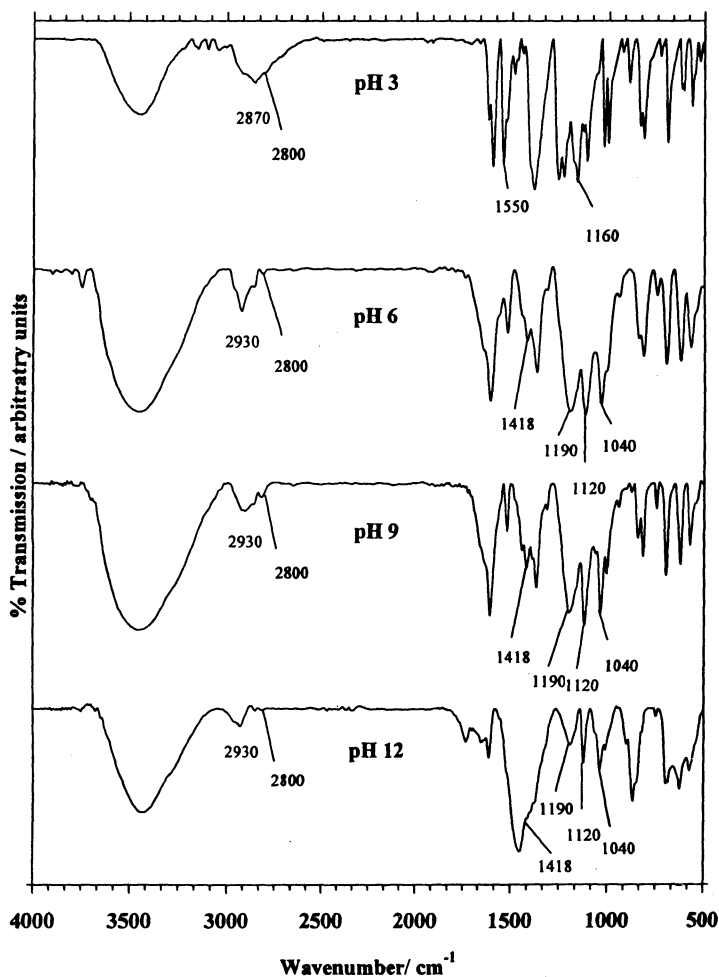


Fig. 3. FTIR spectra of methyl orange precipitated at different pH

(pH 3). The appearance of band at 1550 cm^{-1} , which appeared to be N—H group for acid precipitate solution, verified that the dye structure had changed from the benzenoid structure to the quinoid structure. The bands at 1040 , 1120 and 1190 cm^{-1} for pH 6, 9 and 12, respectively represent the aromatic sulphonic acid salt. Methyl orange at pH 3 did not show the existence of these bands but the appearance of a band at 1160 cm^{-1} is due to the symmetrical stretch of anhydrous sulfonic group. This change of sodium sulfonic salt at pH 3 is confirmed by strong broad band near 2870 cm^{-1} which represents the hydroxyl in the anhydrous sulfonic group. The band at $2810\text{--}2790\text{ cm}^{-1}$ which belongs to aromatic dimethylamine group could also be seen for all the pH.

Electrochemical characterization: The photoelectrochemical behaviour of the thin film was characterized in 10 ppm methyl orange solution. The dye solution was added with 0.1 M NaCl as the supporting electrolyte. The obtained linear sweep voltammogram as shown in Fig. 4 clearly presents the effect when the electrode is intermittently illuminated. The light and dark effect was obtained by manually chopping the irradiation path. The photocurrent response is more obvious and significant towards the more positive potential. This indicates that the minority carrier concentration, hole in this case, was enhanced under illumination and was forced toward the surface under anodic polarization where the oxidation process took place. This explanation suggests that the electron is the major carrier and the TiO_2 obtained is of n -type²³.

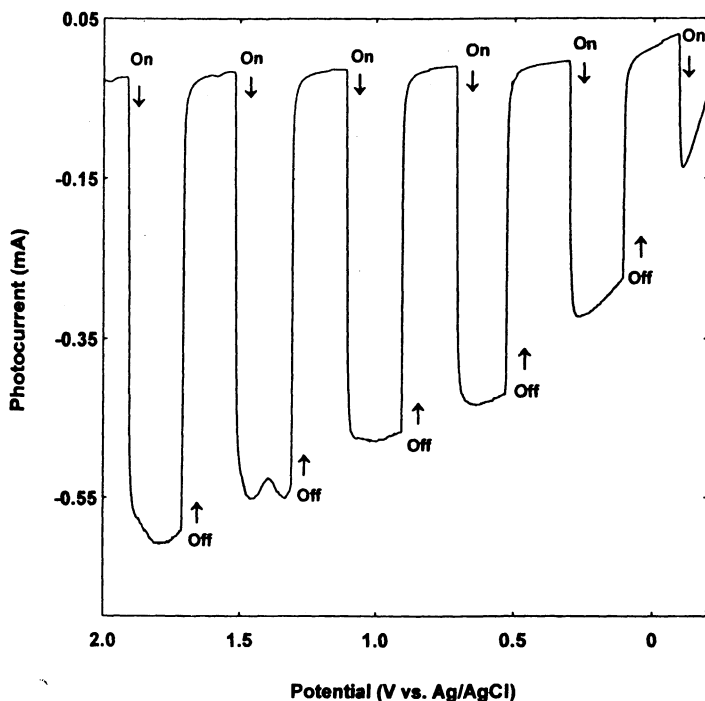


Fig. 4. Photocurrent generation from TiO_2 electrode upon illumination (\downarrow light switching on and \uparrow light switching off)

The behaviour of the electrode at different pH was investigated (Fig. 5) from I-V curves for both dark and under illumination. It is well known that the flat-band potential, E_{fb} shifts by about -59 mV for each unit increase in pH as shown by the equation:

$$E_{fb} = E_{fb}^0 - 0.05916 \text{ pH} \tag{1}$$

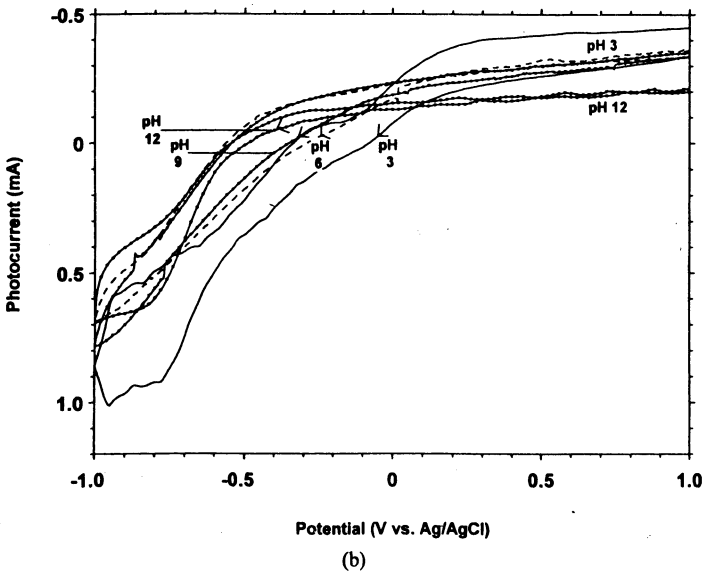
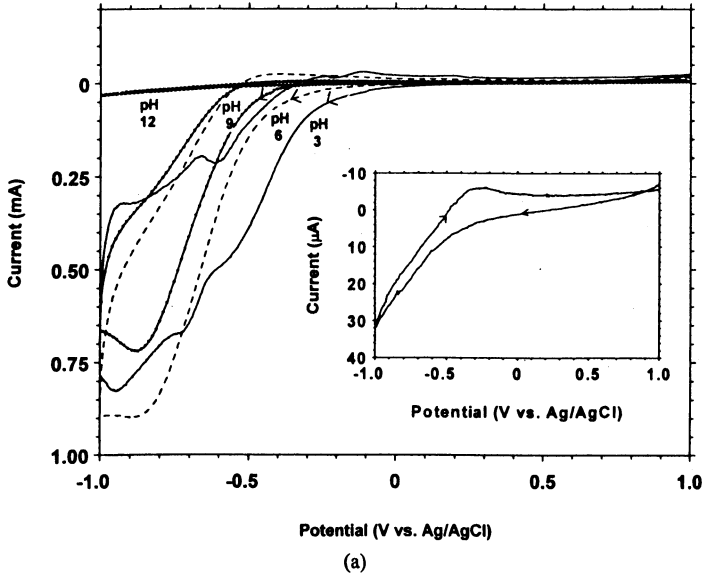


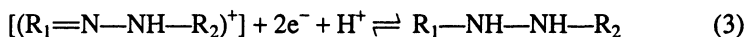
Fig. 5. Current-potential curves of methyl orange (10 ppm and containing 0.1 M NaCl): (a) in dark, inset shows I-V curves for solution at pH 12, (b) with illumination

The photocurrent onset potential techniques could be used to determine the flat band potential of TiO_2 ²⁴. The flat band potentials were shifted to more negative potential by increasing the solution pH. It is also observed that the cathodic dark current at pH 12 is extremely low. As reported by Kesselman *et al.*²⁵, the cathodic current in dark was due to the reduction of water which occurred at potential -0.83 V (*vs.* SHE electrode) and the half reaction is shown below:

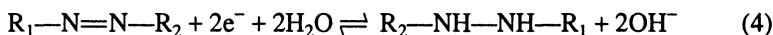


Besides that, the major difference in methyl orange structure at different pH is on azo groups as discussed previously²⁶. The mechanisms of the reduction of azo group dyes at acidic and basic media would also be different. In acidic medium, two electrons process occurred on pre-protonated azo groups eq. (3). In alkaline medium, reduction of dye also involved 2 electrons but this reaction is far thermodynamically unfavourable (eqn. (4)).

Acid medium:

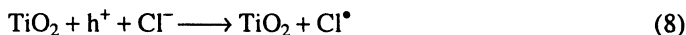
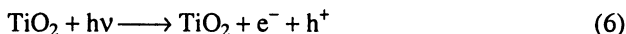
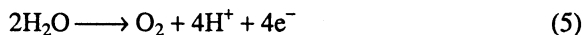


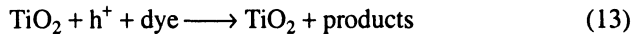
Alkaline medium:



From the above equations, it is clear that the pre-protonated azo dye in strong acidic media is easier to reduce. This agrees with the literature report that azo group dyes are more readily reduced in strongly acidic media²¹. On the other hand, the reduction of azo groups in high alkaline media is very difficult to occur which resulted in extremely low current.

Under illumination, the magnitudes of the anodic current are quite similar for pH 3, 6 and 9 while pH 12 shows a weakest current response. However, the latter exhibit stronger cathodic current compared to the dark. At the anodic side, the photocurrents are mainly attributed to generation of radicals and oxidation of water or dye. In this system, the anions in the solution will react with the holes to produce strong oxidizing radicals such as OH^\bullet and Cl^\bullet . These radicals attack and oxidize the dye molecules. These reactions could be represented by the following equations:





Thus, lower anodic photocurrent for solution at pH 12 means the reactions represented by eqs. (5) to (13) are comparatively less.

Photoelectrocatalytic degradation experiment: Photodegradation of most of the organic pollutants are widely influenced by pH. It is an important parameter to be investigated, particularly in attempting to introduce and apply this method on wastewater treatment. The influence of pH on the photoelectrocatalytic degradation rate of methyl orange is shown in Fig. 6. The experimental results are reported as ratio of C/C_0 vs. illumination time (t), where C_0 is the initial concentration of dye and C is the concentration at t minutes. The photodegradation process was found to follow the pseudo-first order kinetic reaction. The values of pseudo first order rate constant, correlation factor and percentage of photoelectrocatalytic degradation of methyl orange are given in Table-1 and Fig. 5 (inset) respectively. It is clearly shown that the degradation rate is higher in near neutral (natural dye pH) than acidic or alkaline condition. However, acidic media show rather high photodegradation percentage compared to strong alkaline medium (pH 12).

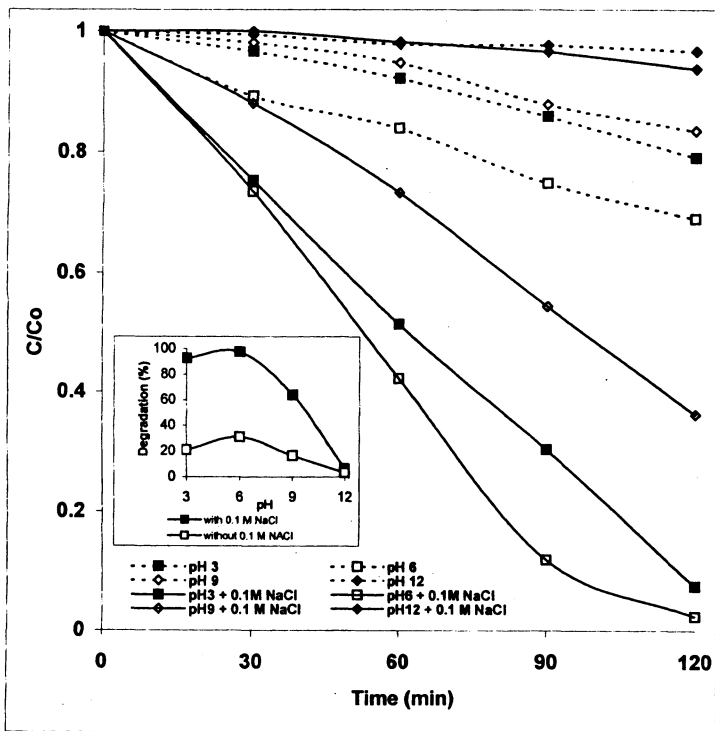


Fig. 6. The methyl orange degradation rate dependence on pH for solution with and without added with supporting electrolyte (0.1 M NaCl). Inset shows comparison in terms of degradation percentage

TABLE-1
PSEUDO FIRST ORDER KINETIC RATE CONSTANTS AND HALF TIMES OF
PHOTOELECTROCATALYTIC DEGRADATION OF METHYL ORANGE AT
DIFFERENT SOLUTION pH

pH	Without supporting electrolyte			With supporting electrolyte		
	$k \times 10^{-3}$ (min^{-1})	$t_{1/2}$ (min)	R^2	$k \times 10^{-3}$ (min^{-1})	$t_{1/2}$ (min)	R^2
3	2.0	346.5	0.97	20.4	34.0	0.94
6	3.1	223.6	0.99	31.1	22.3	0.93
9	1.6	433.1	0.95	8.4	82.5	0.95
12	0.3	2310.0	0.96	0.5	1386.0	0.94

It is well known that the surface of TiO_2 is amphoteric and consequently the charge of the surface is pH dependent. The point of zero charge (pH_{zpc}) for TiO_2 is close to 6²⁷. Therefore, at low pH value, the TiO_2 surface is positively charged which induces an increase of the adsorption of negatively charged sulphonate group of methyl orange. Hence in acidic pH range, this electrostatic interaction between both opposite charge species leads to high rate of degradation. In alkaline medium at pH 9 and 12, both TiO_2 and dye anion surfaces acquire negative charge which retards adsorption. Consequently, the degradation rate is slower especially for highly alkaline medium at pH 12. However, the electrostatic interaction due to the surface charging does not affect the electrochemical degradation where near neutral pH (pH 6) shows the highest photodegradation rate. This is due to the fact that the potential applied (1.0 V) is more positive than the flat band potential of TiO_2 . Thus, the effect of pH_{zpc} could be eliminated since the surface charge always becomes positive by the formation of a depletion layer ($n\text{TiO}_2$).

The explanation of effect of pH on the photodegradation may sometimes take a different approach. For example, the photodegradation rate of acid orange was reported higher in alkaline than in acidic medium²⁸. The increase in degradation rate at higher pH value was attributed to generation of more hydroxyl radicals at high OH^- concentration. Nevertheless, in this electrochemical assisted photodegradation system, neither acidic nor basic pH medium is favourable for photodegradation of methyl orange. Therefore, it is possible to infer that the variation in the rate at different pH for an electrochemical assisted system is mainly due to photodegradation mechanisms.

As discussed, the flat band potential decreases about 59 mV per pH unit. Consequently, the negative shift in E_{fb} with increasing pH results in diminished oxidative power of the holes²⁹. This will bring differences in the kinetics and mechanism of the electrode reaction. Thus, the amount of hydroxyl radicals is not linearly dependent on the concentration of hydroxyl ions. This explains the low current and low photoelectrocatalytic degradation rate obtained at pH 12 as shown in Fig. 5 (b) and Fig. 6, respectively. The reason for near neutral pH shows the highest degradation rate probably due to the shift of optimum flat band potential for the formation of OH^\bullet , Cl^\bullet and $\text{Cl}^{\bullet-}$ radicals.

Roles of supporting electrolyte: From Fig. 6, it can be seen that the addition of chloride ions as supporting electrolyte significantly promotes the photoelectrocatalytic degradation rate. It is worth noting that the degradability trend is the same for the medium in presence and absence of supporting electrolyte. The chloride ion will be oxidized to generate the Cl^\bullet and $\text{Cl}_2^{\bullet-}$ radicals [eqns. (8) and (9)] which is favourable for photoelectrocatalytic degradation process. This could be observed by significant increases of photodegradation rate at pH 3, 6 and 9 compared to the solution without the supporting electrolyte. However, the photoelectrocatalytic degradation at pH 12 is still the same although with the addition of the supporting electrolyte. This is because the competition of chloride ions with hydroxyl ions to be adsorbed on TiO_2 could be ignored in high alkaline media. Thus, hydroxyl ions are dominant in the solution at this pH. Nevertheless, the limitation factor of low oxidative power of holes due to the shifting of flat band potential contributed to low photodegradation rate.

Hepel and Luo²⁹ had reported that pH is a key factor in the elucidation of the reaction mechanism on the electrode. This suggested that the supporting electrolyte only plays a small part in the reaction mechanism by producing the chloride radicals. This is proved by the same trend of photodegradation ability for all pH. The main function of supporting electrolyte is providing the conducting medium for the transportation of dye species in bulk solution to the electrode surface, which is essential in an electrochemical assisted system. The addition of supporting electrolyte minimizes uncompensated iR drop, which leads to potential-control error and also minimizes the ohmic heating of the solution³⁰.

The decrease of absorbance value is rather faster for the solution added with supporting electrolyte. Besides that, the red shift of λ_{max} of the spectrum could be observed for solutions without a supporting electrolyte. This indicates that the solution acidity increases during the photoelectrochemical degradation process. In this case, the presence of supporting electrolyte helped to buffer the solution by reacting with the OH^- or H^+ produced in the solution as shown by eqns. (2) and (5).

Conclusion

The results confirmed the changes of methyl orange structure with protonation at low pH. This caused the dye to exhibit different oxidation and reduction behaviours. The photoelectrocatalytic degradation rate of the dye in near neutral and acidic medium is higher than basic medium. The low degradation rate by decreasing the solution acidity is due to the decrease of oxidative power of holes as identified by the shift in the flat band potential. Presumably, a solution at near neutral pH provides the optimum potential for TiO_2 to generate the oxidant species which resulted in high photoelectrocatalytic degradation rate. The presence of supporting electrolyte did not affect the photodegradation trends but significantly promoted the rate. In addition, the supporting electrolyte enhance the ionic conduction in the electrolyte as well as buffering the solution.

ACKNOWLEDGEMENT

Authors gratefully acknowledge the financial support from the Malaysian Government through IRPA No: 09-02-04-0255-EA001 and 09-02-04-0369-EA001.

REFERENCES

1. H. Zollinger, *Color Chemistry: Synthesis, Properties and Applications of Organic Dyes and Pigments*, VCH Publishers, New York, p. 86 (1987).
2. H.M. Pinheiro, E. Touraud and O. Thomas, *Dyes and Pigments*, **61**, 121 (2004).
3. F. Kiriakidou, D.I. Kondarides and X.E. Verykios, *Catal. Today*, **54**, 119 (1999).
4. M.R. Hoffman, S.T. Martin, W.Y. Choi and D.W. Bahnemann, *Chem. Rev.*, **95**, 69 (1995).
5. D.A. Tryk, A. Fujishima and K. Honda, *Electrochim. Acta*, **45**, 2363 (2000).
6. J. Luo and M. Hepel, *Electrochim. Acta*, **46**, 2913 (2001).
7. G. Sivalingam, K. Nagaveni, M.S. Hegde and G. Madras, *Appl. Catal. B: Environ.*, **45**, 23 (2003).
8. A. Fujishima, T.N. Rao and D.A. Tryk, *J. Photochem. Photobiol. C: Photochem. Rev.*, **1**, 1 (2000).
9. A.L. Linsebigler, G. Lu and J.T. Yates. (Jr.), *Chem. Rev.*, **95**, 735 (1995).
10. K. Vinodgopal, S. Hotchandani and P.V. Kamat, *J. Phys. Chem.*, **97**, 9040 (1993).
11. K. Vinodgopal, U. Stafford, K.A. Gray and P.V. Kamat, *J. Phys. Chem.*, **98**, 6797 (1994).
12. X.Z. Li, F.B. Li, C.M. Fan and Y.P. Sun, *Wat. Res.*, **36**, 2215 (2002).
13. H. Hidaka, T. Shimura, K. Ajioka, S. Horikoshi, J. Zhao and N. Serphone, *J. Photochem. Photobiol. A: Chem.*, **109**, 165 (1997).
14. R. Pelegrini, P.P. Zamora, A.R. Andrade, J. Reyes and N. Duran, *Appl. Catal. B: Environ.*, **22**, 83 (1999).
15. G. Waldner, M. Pourmodjib, R. Bauer and M. Neumann-Spallart, *Chemosphere*, **50**, 989 (2003).
16. K. Kato, A. Tsuzuki, Y. Torii and H. Taoda, *J. Mater. Sci.*, **30**, 837 (1995).
17. K. Kato, A. Tsuge and K. Niihara, *J. Am. Ceram. Soc.*, **79**, 1483 (1996).
18. K. Kato and K. Niihara, *Thin Solid Films*, **298**, 76 (1997).
19. G. Calvert and J.N. Pitts (Jr.), in: *Photochemistry*, John Wiley & Sons, New York, pp. 452 (1967).
20. R.L. Cisneros, A.G. Espinoza and M.I. Litter, *Chemosphere*, **48**, 393 (2002).
21. X. Peng and J. Yang, *Dyes and Pigments*, **20**, 73 (1992).
22. N.B. Colthup, L.H. Daly and S.E. Wiberley, *Introduction to infrared and Raman spectroscopy*, 2nd Edn., Academic Press, New York, Ch. 11 (1975).
23. S.E. Lindquist, B. Finnstorm and L. Tegner, *J. Electrochem. Soc.*, **130**, 351 (1983).
24. H.O. Finklea, *Semiconductor Electrodes*, Elsevier, Netherlands, pp. 30–31 (1988).
25. J.M. Kesselman, N.S. Lewis and M.R. Hoffman, *Environ. Sci. Tech.*, **31**, 2298 (1997).
26. M.V.B. Zanoni, P.A. Carneiro, M. Furlan, E.S. Duarte, C.C. Guaratini and A.G. Fogg, *Anal. Chim. Acta.*, **385**, 385 (1999).
27. X. Domenech and J. Peral, *Chemosphere*, **38**, 1265 (1999).
28. F. Kiriakidou, D.I. Kondarides and X.E. Verykios, *Catal. Today*, **54**, 119 (1999).
29. D.T. Sawyer and J.R. Roberts, *Experimental for Chemists*, Wiley-Interscience, New York, p. 167 (1974).